

Early Risk Prediction of Pediatric Cardiac Arrest from Electronic Health Records via Multimodal Fused Transformer

Jiaying Lu^{*1}, Stephanie R. Brown^{*2}, Songyuan Liu¹, Shifan Zhao³, Kejun Dong¹, Del Bold¹, Michael Fundora², Alaa Aljiffry², Alex Fedorov¹, Jocelyn Grunwell² and Xiao Hu^{1,4}

Abstract—Early prediction of pediatric cardiac arrest (CA) is critical for timely intervention in high-risk intensive care settings. We introduce PEDCA-FT, a novel transformer-based framework that fuses tabular view of EHR with the derived textual view of EHR to fully unleash the interactions of high-dimensional risk factors and their dynamics. By employing dedicated transformer modules for each modality view, PEDCA-FT captures complex temporal and contextual patterns to produce robust CA risk estimates. Evaluated on a curated pediatric cohort from the CHOA-CICU database, our approach outperforms ten other artificial intelligence models across five key performance metrics and identifies clinically meaningful risk factors. These findings underscore the potential of multimodal fusion techniques to enhance early CA detection and improve patient care.

I. INTRODUCTION

Cardiac arrest (CA) in the pediatric population is a critical and life-threatening event with significant implications for morbidity and mortality [1]. While less common than in adults, pediatric CA is often associated with a preceding period of physiological instability, making timely identification and intervention crucial. Many cases of CA in children occur in intensive care units (ICUs) [2], particularly cardiac ICUs [3], where children with congenital or acquired heart diseases are managed. In these high-stakes environments, the interplay of complex cardiac conditions, surgical interventions, and critical care therapies, coupled with significant cognitive and data overload, creates a unique set of challenges for clinicians [4]. Early prediction of CA [5] in this setting could enable proactive measures to prevent arrests and provide situational awareness. This underscores the importance of developing robust predictive models tailored to the pediatric cardiac ICU population, integrating clinical, physiological, and potentially novel data sources.

Electronic Health Records (EHRs) offer a rich repository of patient data [2], making them an attractive resource for cardiac arrest risk prediction. By aggregating diverse information such as demographics, vital signs, laboratory results, and clinical notes, EHRs provide a comprehensive view of a patient’s health trajectory. However, leveraging

EHR data for pediatric CA risk prediction is not without challenges [6]. First, EHRs are inherently *heterogeneous*[†], encompassing various modalities that differ in format and clinical significance. For examples, demographics are stored in the static categorical format that serve as underlying risk factors, whereas vital signs are recorded as longitudinal numerical measurements that reflect short term physiological status. Second, EHR data are *multi-resolution*: some measurements, like vital signs, are updated in near real-time, while others, such as lab results, are recorded at more sparse intervals. Traditionally, clinicians have relied on manually developed criteria and scoring systems (e.g., PEWS [7], IDO2 [8]) to predict cardiac arrest. While these systems are valuable, they may not fully capture the subtle, individual-specific nuances of a patient’s condition because they depend on universally predefined thresholds applied to a fixed set of clinical observations. Moreover, certain systems, such as IDO2, are proprietary, limiting their accessibility without incurring additional costs. In contrast, data-driven approaches leverage EHR data through advanced artificial intelligence (AI) techniques, leading to improved performance in early detection and risk stratification of pediatric cardiac arrest [5].

The heterogeneous and multi-resolution nature of EHR poses significant challenges to AI models for EHR-based pediatric CA risk prediction. Conventional AI models (e.g., random forest, XGBoost [9]), which are designed for static tabular data, excel at handling high-dimensional numerical and categorical risk factors by capturing subtle and non-linear patterns indicative of impending cardiac arrest. However, these models operate on fixed-dimensional input features and typically require ad-hoc, domain-specific feature preprocessing—such as aggregation [10]—which can overlook important dynamic temporal changes in risk factors. On the other hand, time-series AI models [11] are well-suited for analyzing longitudinal data, as they can capture temporal dependencies and trends. Although resolution unification techniques (e.g. resampling, padding, interpolation) [12], [13] can address the multi-resolution challenges inherent in EHR data, time-series models often struggle to effectively handle high-dimensional inputs.

To address the above mentioned challenges, we propose our innovative approach, namely **PEDI**atric Cardiac Arrest

^{*}Corresponding Author: Jiaying Lu, Ph.D. (jiaying.lu@emory.edu)

^{*}These authors contributed equally to this work

¹Center for Data Science, Nell Hodgson Woodruff School of Nursing, Emory University, Atlanta, GA 30322, USA

²Department of Pediatrics, Children’s Healthcare of Atlanta Cardiology, School of Medicine, Emory University, Atlanta, GA 30322, USA

³Department of Mathematics, Laney Graduate School, Emory University, Atlanta, GA 30322, USA

⁴The Wallace H. Coulter Department of Biomedical Engineering, Georgia Institute of Technology & Emory University, Atlanta, GA 30322, USA

[†]Heterogeneous: while many works use the term “multivariate” to refer to the complex input features in the context of time-series models, here we use “heterogeneous” to emphasize two levels of heterogeneity: (1) static versus dynamic risk factors, and (2) categorical, numerical, and textual input formats.

prediction via **Fused Transformer** (PEDCA-FT), based on a novel tabular-textual multimodal fusion strategy [14], [15], and the powerful Transformer backbone model for each modality. We view the heterogeneous and multi-resolution risk factors as two complementary modalities, tabular and textual, each characterized by its own intrinsic data structure. Specifically, we employ a dedicated tabular Transformer [16], [17] to effectively handle high-dimensional static and aggregated longitudinal tabular features, while a pre-trained textual EHR Transformer [18] processes the textual representations [19] derived from the original EHR data. A fusion Transformer is then used to integrate the modality-specific representations, ultimately computing the probability of CA onset risk. We evaluate the effectiveness of our PEDCA-FT on a curated cohort from the CHOA-CICU database comprising 3,566 pediatric patients with a 4.0% incidence of CA. Our model, along with ten other AI models, is compared using 5-fold cross-validation. Through this comprehensive evaluation, our proposed approach marginally outperforms all compared models. Furthermore, a feature importance analysis reveals that several of the identified risk factors align well with clinical knowledge for pediatric CA, as confirmed by our clinical collaborators.

II. STUDY DESIGN

A. Problem Definition

We are interested in the early risk prediction of cardiac arrest for pediatric ICU population.

Definition 1 (Patient EHR Data): The EHR data \mathbf{x} of one patient include static risk factors $\mathbf{x}^{(s)} \in \mathbb{R}^{d_s}$ during one admission such as demographics and admission diagnosis, and temporal risk factors $\mathbf{x}_{0:T}^{(t)} \in \mathbb{R}^{d_t \times T}$ such as patient’s lab results, vital signs, and nursing assessments. Therefore, the EHR data within first τ hours is defined by $\mathbf{x}_{t \leq \tau} = (\mathbf{x}^{(s)}, \mathbf{x}_{0:\tau}^{(t)})$, and $|\mathbf{x}|$ denotes overall number of risk factors contained in EHR data.

Definition 2 (Early Risk Prediction of Cardiac Arrest):

We aim to employ a predictive model $f_\theta(\cdot)$ using a patient EHR data $\mathbf{x}_{t \leq \tau}$ available in the first τ hours of admission, to predict the probability of developing cardiac arrest $\hat{y} = f_\theta(\mathbf{x}_{t \leq \tau})$, where $\hat{y} \in \{0, 1\}$ during the rest of the admission stay.

B. Data Source and Cohort Selection

CHOA-CICU database is a private pediatric intensive care database extracted from electronic health record for all pediatric patients (age less than 18 years) admitted from 1/1/2018 to 12/31/2023 to a large, quaternary, academic Pediatric Cardiac Intensive Care Unit (CICU) at Children’s Hospital at Atlanta and Emory University. We obtain 9 static risk factors from CHOA EHR, including: “gender, ethnicity, first race, second race, primary language, respiration distress, age, admission diagnoses, admission ICD 19 codes”. Among 184 temporal risk factors, we obtain 129 vital signs and nursing assessments from flow sheet after removing non-relevant items and removing missing rate > 0.5 items. We also obtain 49 lab test results after removing missing rate

> 0.5 items, and 5 medications after removing missing rate > 0.7 items. Table I briefly presents the number of patients included in the two data sources.

TABLE I: Statistics of CICU patients After Cohort Selection.

Category	Value
Patient, no. (% of case)	3,566 (4.0%)
Admissions, no. (% of case)	4,672 (3.1%)
Age, median years (Q1–Q3)	0.6 (0.1 – 5.5)
Gender, no. of female (%)	1,676 (47.0%)
CICU LoS, median days (Q1–Q3)	8.4 (4.3 - 20.0)
HLoS, median days (Q1–Q3)	2.0 (0.9 - 5.2)
Mortality, no., (% of Admission)	185 (4.0%)
Static Risk Factors, no.	9
Temporal Risk Factors, no.	184
-(Tempo) Vital&Assessments, no.	129
-(Tempo) Lab Results, no.	49
-(Tempo) Medications, no.	5

III. METHODS

The two major challenges we face are (1) the large feature space due to the multimodal, heterogeneous patient risk factors; (2) the label imbalance due to the low prevalence of CA in pediatric CICU patients. Our proposed model, PEDCA-FT, is a multimodal transformer late-fusion model, which utilize both raw structured EHR features (tabular) and derived textualized EHR features (textual) as input. As can be seen in Fig. 1, PEDCA-FT consists of three modules: tabular-transformer \mathcal{T}_{tab} , pre-trained textual-transformer \mathcal{T}_{txt} , and fusion-transformer \mathcal{T}_{fus} . The tabular-transformer is corresponding to obtain latent representation from patient’s raw EHR data, denoted by $\mathbf{h}_{tab} = \mathcal{T}_{tab}(\mathbf{x}_{t \leq \tau})$. The textual-transformer is corresponding to obtain latent representation from patient’s textualized EHR data, denoted by $\mathbf{h}_{txt} = \mathcal{T}_{txt}(g(\mathbf{x}_{t \leq \tau}))$ where $g(\cdot)$ denotes the textualization function for EHR. After obtaining latent representations from two views, we utilize the fusion-transformer to predict the likelihood of cardiac arrest, denoted by $\hat{y} = \mathcal{T}_{fus}(\mathbf{h}_{tab}, \mathbf{h}_{txt})$.

A. Tabular Transformer

Tabular models (*e.g.* XGBoost [9], LightGBM) have demonstrated excessive performance in EHR-based risk predictions. Here, we also employ a tabular view to handle the numerical and categorical risk factors that widely exist in the EHR. We follow the common practice to preprocess these tabular features, where numerical ones are passed through without change and categorical ones are encoded as monotonically increasing integers. For the static risk factors $\mathbf{x}^{(s)}$, we keep them as the original format. For the temporal risk factors, aggregation process is needed to accommodate the input format requirements. Therefore,

$$\mathbf{x}_{agg}^{(t)} = \phi(\mathbf{x}_{0:\tau}^{(t)}), \quad (1)$$

where $\phi : \mathbb{R}^{d_t \times \tau} \rightarrow \mathbb{R}^{d_t}$ denotes the aggregation operator that maps the time-series features into tabular features. A wide range of aggregation operation can be used for ϕ , and we opt to $LAST(\cdot)$ which keeps the last observed element from the whole time-series. The input of tabular-transformer \mathcal{T}_{tab} is $\mathbf{x}_{t \leq \tau} = (\mathbf{x}^{(s)}, \mathbf{x}_{agg}^{(t)})$ after applying Eq. (1).

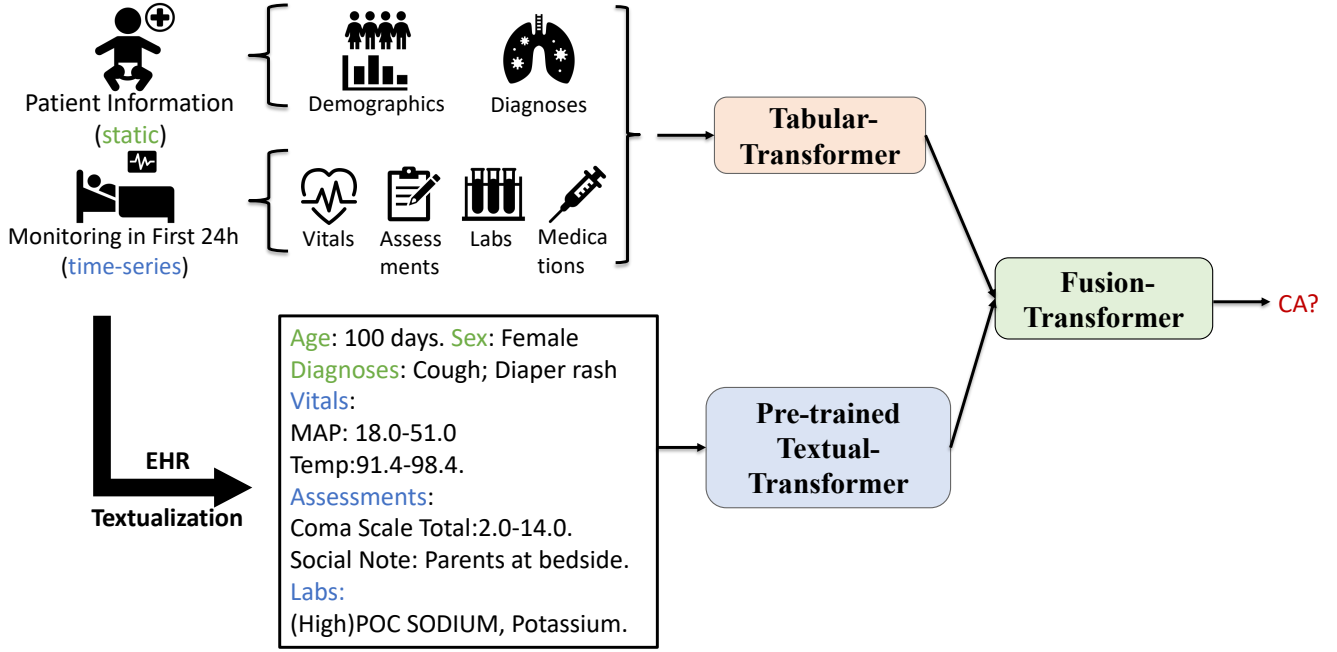


Fig. 1: Model Architecture of PEDCA-FT.

We adapt a tabular feature oriented Transformer [16], [17] variation as our tabular view. In a nutshell, the numerical and categorical inputs are first transformed to dense embeddings and then feed into a stack of Transformer layers. The dense embedding for i -th factor $x_{(i)} \in \mathbb{X}_i$ of $\mathbf{x}_{t \leq \tau}$ is computed by

$$\mathbf{e}_{(i)} = \xi_{(i)}(x_{(i)}) + \mathbf{b}_{(i)}, \quad (2)$$

where $\mathbf{e}_{(i)}(\cdot) \in \mathbb{R}^d$ is i -th the transformed dense embedding, $\xi_{(i)} : \mathbb{X}_{(i)} \rightarrow \mathbb{R}^d$ is the i -th transformation function, and $\mathbf{b}_{(i)} \in \mathbb{R}^d$ is i -th feature transformation bias. Specifically, we implement $\xi_{(i)}(\cdot)$ as the element-wise multiplication

$$\xi_{(i)}(x_{(i)}^{num}) = x_{(i)}^{num} \cdot \mathbf{W}_{(i)}^{num} \quad (3)$$

with the learnable vector $\mathbf{W}_{(i)}^{num} \in \mathbb{R}^d$ for numerical format features, and $\xi_{(i)}$ as the categorical embedding lookup

$$\xi_{(i)}(x_{(i)}^{cat}) = \mathbf{W}_{(i)}^{cat} \mathbb{1}(x_{(i)}^{cat}) \quad (4)$$

with one-hot encoding function $\mathbb{1}(\cdot) : \mathbb{X}_{(i)} \rightarrow \mathbb{R}^d$ and the lookup table $\mathbf{W}_{(i)}^{cat} \in \mathbb{R}^{c_i \times d}$. Overall,

$$\mathbf{e}_{tab} = \text{stack}(\mathbf{e}_{(1)}^{num}, \dots, \mathbf{e}_{(|\mathbf{x}^{num}|)}^{num}, \mathbf{e}_{(1)}^{cat}, \dots, \mathbf{e}_{(|\mathbf{x}^{cat}|)}^{cat}), \quad (5)$$

where $\mathbf{e}_{tab} \in \mathbb{R}^{|\mathbf{x}| \times d}$. Then, L standard general Transformer layers $\mathcal{F}_1, \dots, \mathcal{F}_L$ are applied

$$\mathbf{h}_k = \mathcal{F}_k(\mathbf{h}_{k-1}) \quad (6)$$

with $\mathbf{h}_0 = \mathbf{e}_{tab}$ and $\mathbf{h}_L \in \mathbb{R}^{h_{tab}}$. Please refer to the original paper [20] for technical details of the multi-head self-attention of transformer layer \mathcal{F} .

B. Textual Transformer

The drawback of tabular view is that the aggregation process simplifies the time-series risk factors. We propose a textual view to fully capture the trend and change of these time-series risk factors by presenting their value ranges. Moreover, the static risk factors can also be effectively captured by directly presenting them in the textual format. A pre-trained textual-transformer \mathcal{T}_{txt} is employed to obtain the latent embedding of the textualized EHR data $\mathbf{D} = g(\mathbf{x}_{t \leq \tau})$. In general, the textualized representation of i -th factor $x_{(i)} \in \mathbb{X}_i$ of $\mathbf{x}_{t \leq \tau}$ is computed by

$$\mathbf{D}_{(i)} = g_{(i)}(\mathbf{x}_{(i)}), \quad (7)$$

where $g_{(i)}(\cdot)$ is the i -th textualization function, and $D_{(i)}$ denotes a sequence of length $|D_{(i)}|$ textual tokens $\{d_1, d_2, \dots, d_{|D_{(i)}|}\}$. Specifically, we implement $g_{(i)}(\cdot)$ using the following template for static feature $x_{(i)} \in \mathbb{X}_{(i)}$

$$g_{(i)}(x_{(i)}) = \text{factorName}(x_{(i)}) \# \text{":"} \# x_{(i)} \quad (8)$$

with $\text{factorName}(\cdot)$ denotes retrieving the factor name of $x_{(i)}$, and $\#$ denotes text concatenation function. For instance, $g_{(i)}(x_{(i)}) = \text{"Gender: Female"}$ when $x_{(i)} = \text{"Female"}$ indicating the patient's gender. Moreover, we implement $g_{(i)}(\cdot)$ using the following template for variable length time-series feature $\mathbf{x}_{(i),0:\tau}$

$$g_{(i)}(\mathbf{x}_{(i),0:\tau}) = \text{factorName}(\mathbf{x}_{(i)}) \# \text{":"} \# \begin{cases} \text{set}(\mathbf{x}_{(i),0:\tau}), & \text{if } \mathbf{x}_{(i)} \text{ is categorical} \\ \text{min-max}(\mathbf{x}_{(i),0:\tau}), & \text{otherwise,} \end{cases} \quad (9)$$

where we keep all distinct values of each categorical time-series risk factor, and value min-max range of each numerical time-series factor. As an illustration, for categorical time-series risk factor *skin color*, the textualized result is "Skin

Color: Pink; Pale.” which covers all recorded values. Similarly, for numerical time-series risk factor *body temperature*, the textualized result is “Body Temp: 91.4–98.4.”. With the help of proposed textualization process, the heterogeneous multimodal EHR data is represented into a unified textual format which can be effectively handled by textual transformer, capturing dynamic trend of time-series.

Pre-trained on massive textual corpus that covers public EHR databases, transformer-based models have shown promising in adults-centered risk prediction tasks [21], [22], [23]. We employ a standard bidirectional encoder-only transformer (*i.e.*, BERT [24]) for the pediatric cardiac arrest prediction, since it essentially is a sequence prediction problem after textualization of EHR. Follow the common practice, we add a special sequence token “[CLS]” at the beginning of the converted text, which is used as the text-view representation of one patient’s EHR,

$$\mathbf{h}_{BERT} = \text{BERT}([\text{CLS}], \mathbf{D}), \quad (10)$$

where $\mathbf{h}_{BERT} \in \mathbb{R}^{(|\mathbf{D}|+1) \times d_{txt}}$ and $\text{BERT}(\cdot)$ denotes the employed bi-directional transformer model. It is worth noting that BERT here is different from the multi transformer layer in Eq. (6), since $\text{BERT}(\cdot)$ contains additional word embedding layer and its all learnable parameters are pre-trained. We use the “[CLS]” corresponding embedding as the text-view embedding of textualized EHR, thus $h_{txt} = h_{BERT}[0, :] \in \mathbb{R}^{d_{txt}}$. One technical challenge for our textual transformer module is the maximum sequence length. To accommodate with that constraint, we further polish the textualization function $g(\cdot)$ for time-series laboratory test results. Inspired by the clinical decision making process that paying more attentions to abnormal findings [25], we filter out laboratory results that fall into the normal reference range and only keep the names of abnormal ones. Therefore, an example of textualized laboratory results can be “(High) Sodium; Potassium. (Low) Glucose.”. Furthermore, we add section headers, including “Demographics”, “Vitals”, “Assessments”, “Labs” and “Medications”, for each covered EHR table, as can be seen in the toy example of Fig. 1. These above ad-hoc design aims to make the textualized EHR more readable and concise for the textual-transformer.

C. Fusion Transformer

After obtain the view-specific dense representation of patient EHR from tabular-transformer by $\mathbf{h}_{tab} = \mathcal{T}_{tab}(\mathbf{x}_{t \leq \tau})$ and textual transformer by $\mathbf{h}_{txt} = \mathcal{T}_{txt}(g(\mathbf{x}_{t \leq \tau}))$, we utilize a late-fusion strategy [14], [15] to calculate the final probability of the pediatric patient’s cardiac arrest onset. We still use the powerful Transformer architecture as the major technical component, with a concatenation operation to pool the two representations

$$\hat{p} = \text{sigmoid}(W(\mathcal{F}_{1:M}(\mathbf{h}_{tab}, \mathbf{h}_{txt})) + b), \quad (11)$$

where $\hat{p} \in [0, 1]$ denotes the predicted probability of CA onset, $\mathcal{F}_{1:M}(\cdot)$ denotes the multiple transformer layers, and $W(\cdot) + b$ denotes the last prediction layer.

The focal loss [26] is used to train the three modules of PEDCA-FT to deal with the class imbalance (CA incidence=3.1%)

$$FL(p_{true}) = -(1 - p_{true})^\gamma \log(p_{true}), \quad (12)$$

where

$$p_{true} = \begin{cases} \hat{p}, & \text{if } y = 1, \\ 1 - \hat{p}, & \text{otherwise,} \end{cases} \quad (13)$$

and γ is a hyperparameter focusing on reduce the loss contribution from well-classified examples ($p_{true} \approx 1$).

IV. EXPERIMENTAL RESULTS

A. Experimental Settings

We use our curated cardiac arrest cohort from CHOA-CICU to conduct 5-fold cross-validation. We further ensure that no patient appears in both the training and testing sets for an unbiased evaluation. As defined in Sec. II, our research problem, early risk prediction of CA, is formulated as a binary classification task. Accordingly, we employ a broad set of binary classification metrics, including balanced accuracy (Bal_Acc), F1 score, Matthews Correlation Coefficient (MCC), Area Under the Precision-Recall Curve (AUPRC), and Area Under the Receiver Operating Characteristic Curve (AUROC), to comprehensively assess model performance while accounting for the inherent class imbalance (admission-wise CA incidence = 3.1%). In our evaluation, CA events are treated as the positive class. Among these metrics, Bal_Acc is a specifically designed metric to avoid inflated performance on imbalanced dataset, which is essentially arithmetic mean of sensitivity and specificity in binary classification case. F1 is a harmonic mean of the precision and recall. MCC is defined as

$$\text{MCC} = \frac{tp \times tn - fp \times fn}{\sqrt{(tp + fp)(tp + fn)(tn + fp)(tn + fn)}}, \quad (14)$$

where is generally regarded as a balanced metric for imbalanced case. A MCC of +1 presents a perfect prediction, 0 an random prediction, and -1 an inverse prediction. AUROC and AUPRC both assess trade-offs between key performance rates. While AUROC is widely used—providing a threshold-independent evaluation of the balance between TPR and FPR and serving as a valuable benchmark for comparison with prior work—AUPRC is often more informative in scenarios with class imbalance [27], as it emphasizes the trade-off between precision and recall and focuses on performance for the minority (positive) class.

B. Compared Baseline Models

To comprehensively evaluate the effectiveness of our proposed model, we include ten other AI models. As we summarize before that the EHR data used for pediatric CA is heterogeneous and multi-resolution, the ten AI models can be categories into the following three groups with different EHR feature processing techniques.

TABLE II: Experimental results on CHOA-CICU curated cohort (numbers in percentage).

Model	Bal_Acc	F1	MCC	AUPRC	AUROC
<i>Clinician Derived Risk Scores</i>					
KNN-Dtw	51.65 ± 3.71	2.06 ± 4.61	1.36 ± 3.35	3.81 ± 0.91	55.27 ± 4.21
SVC-Gak	50.00 ± 0.00	0.00 ± 0.00	0.00 ± 0.00	6.19 ± 2.21	54.72 ± 3.80
<i>Last Observed Risk Factors</i>					
KNN-Unif	50.22 ± 0.72	1.18 ± 2.63	1.83 ± 5.62	4.53 ± 1.24	57.41 ± 2.99
LR	49.80 ± 0.77	2.70 ± 1.56	-0.39 ± 1.52	4.60 ± 0.49	62.92 ± 1.92
RF-Gini	50.00 ± 0.00	0.00 ± 0.00	0.00 ± 0.00	7.05 ± 0.81	73.29 ± 2.47
XGBoost	61.03 ± 3.18	11.80 ± 1.96	10.18 ± 2.45	6.88 ± 1.18	72.35 ± 4.00
LightGBM	53.74 ± 5.28	8.62 ± 5.92	5.24 ± 6.96	5.82 ± 2.26	61.42 ± 11.06
TabNN	50.84 ± 0.64	3.90 ± 2.33	1.82 ± 1.68	5.34 ± 0.79	62.16 ± 3.64
<i>Numerical Time-Series Risk Factors</i>					
TResNet	53.93 ± 2.80	10.32 ± 4.54	7.47 ± 4.83	7.53 ± 1.95	72.21 ± 7.22
gMLP	52.51 ± 1.64	8.05 ± 3.54	5.11 ± 3.54	8.72 ± 3.13	75.04 ± 3.52
<i>Our Proposed Tabular-Textual Multimodal Risk Factors</i>					
PEDCA-FT	63.08 ± 3.65	14.31 ± 2.28	13.18 ± 2.55	9.15 ± 3.16	<u>73.99</u> ± 3.16

1) *Clinician Derived Risk Scores*: We use Pediatric Early Warning Score (PEWS) [7] to process EHR data, which involves assessing a range of vital signs and clinical observations—such as heart rate, respiratory rate, blood pressure, oxygen saturation, and behavioral changes—assigning scores based on deviations from normal values, and summing these to produce an overall risk score. The PEWS scores are recorded at various time points by professionals in the EHR, resulting in univariate, variable-length time-series data for each patient. We then employ K-nearest neighbors with dynamic time wrapping [28] (KNN-Dtw) and support vector classifier with global alignment kernel [29] (SVC-Gak). Both dynamic time warping and the global alignment kernel are specifically designed to capture nonlinear similarities in univariate time series of unequal lengths. We implement KNN-Dtw and SVC-Gak based on *tslearn* codebase [30].

2) *Last Observed Risk Factors*: We implement a dedicated aggregation process, *LAST*(\cdot), to transform EHR data into a multivariate static tabular format by capturing the most recent observations of risk factors. This transformation enables the use of a wide range of classical tabular AI models, including KNN with uniform weights (KNN-Unif), logistic regression (LR), random forest with Gini impurity (RF-Gini), extreme gradient boosting (XGBoost) [9], light gradient-boosting machine (LightGBM) [31], and tabular neural network (tabNN) [32]. In this process, numerical features remain unchanged, categorical features are converted into numerical values via ordinal encoding, and missing values are not imputed but are instead assigned a designated NaN value. All tabular models are implemented based on *AutoGluon* codebase [33].

3) *Numerical Time-Series Risk Factors*: We perform a resolution unification process on the EHR data by discretizing the time axis into 1-hour intervals. For each risk factor, repeated recorded values within a 1-hour bucket are aggregated using the *mean*(\cdot) operator. As a result, we obtain 82 distinct numerical time-series features with a fixed length of 24, representing data from the first 24 hours after admission. Categorical risk factors are excluded from this process, as there is no well-defined aggregation operator for them. To capture both the interactions among multivariate

time-series features and their long-term dependencies, we employ state-of-the-art AI models. In particular, we leverage TResNet [34], which utilizes residual convolutional neural networks, and gMLP [35], which is based on a gated multilayer perception architectures. Both deep neural networks are trained with focal loss [26] and are further calibrated with Top-K percentile based best threshold to deal with class imbalance. All time-series deep neural networks are implemented based on *tsai* codebase [36].

C. Experimental Results & Discussion

Table II summarizes the performance of our proposed PEDCA-FT to ten baseline models on various evaluation metrics. Notably, PEDCA-FT achieves the highest Bal_acc, F1, MCC, and AUPRC outperforming all baseline models by an average improvement of 10.71, 9.45, 9.55, and 3.10 separately. Additionally, PEDCA-FT ranks second in AUROC, with an average improvement of 11.57 except for gMLP model. Among baseline models, XGBoost achieves the runner-up in Bal_Acc, F1, and MCC, while gMLP achieves the second best in AUPRC and the highest AUROC. The slightly lower AUROC of PEDCA-FT compared to gMLP can be attributed to AUROC’s emphasis on overall ranking separability, which does not necessarily translate into optimal classification decisions [27], particularly in highly imbalanced datasets. AUROC measures the ability of a model to distinguish between control and case classes across all possible classification thresholds. However, it averages performance across all thresholds and gives equal importance to the classification of both the majority (control) and minority (CA) classes. In highly imbalanced datasets such as the pediatric CA prediction scenario, this can be problematic because the model might perform well on predicting non-CA patients and still achieve a high AUROC, even if it struggles to correctly identify patients at high risk of CA. Furthermore, our results highlight the effectiveness of multimodal data fusion. Models based on tabular representations (i.e., those using last observed risk factors) generally achieve superior Bal_Acc, F1, and MCC, whereas models leveraging time-series representations tend to perform better in AUPRC and AUROC. Integrating a tabular transformer to capture com-

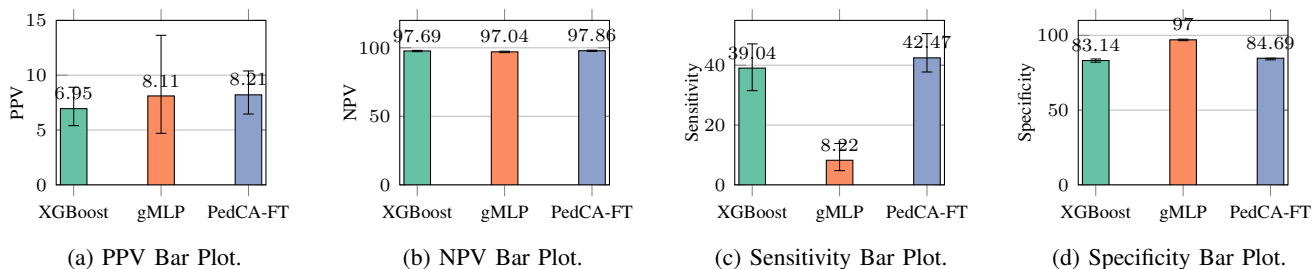


Fig. 2: Bar plots with error bars illustrating PPV, NPV, Sensitivity, and Specificity.

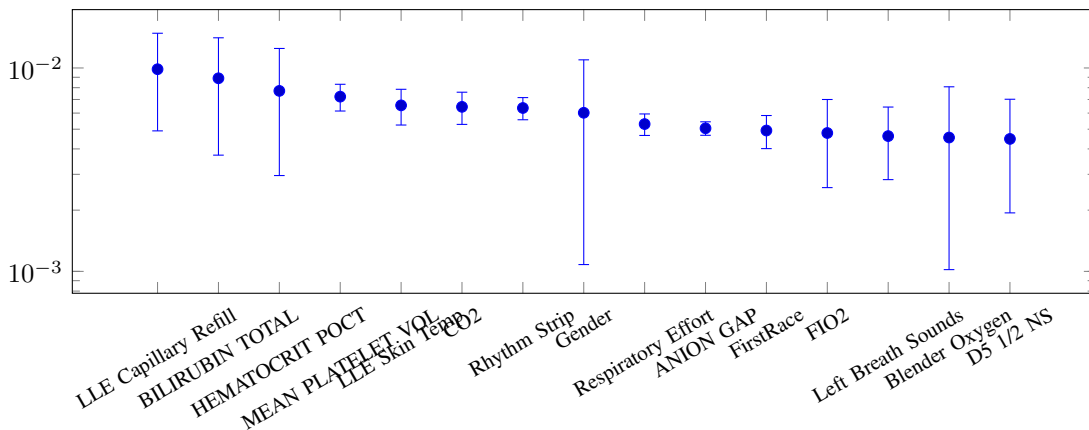


Fig. 3: Feature importance analysis using feature permutation. Error bar indicates p95 high and p95 low.

plex interactions among high-dimensional tabular risk factors and a pre-trained textual transformer to effectively model the dynamics of textualized time-series risk factors, PEDCA-FT delivers SOTA performance for CA risk prediction.

We further analyze XGBoost, gMLP, and PEDCA-FT in terms of Positive Predictive Value (PPV), Negative Predictive Value (NPV), Sensitivity, and Specificity, as shown in Figure 2, to align with clinical priorities. Overall, PEDCA-FT achieves the most balanced performance across all four metrics. Specifically, PEDCA-FT demonstrates a slight advantage in both PPV and NPV, while gMLP exhibits high variance in PPV, as indicated by the wide error bars. Notably, PEDCA-FT attains the highest sensitivity, which is particularly crucial for screening CA, where missing cases can have severe consequences. At the same time, PEDCA-FT maintains competitive specificity, striking a careful balance between sensitivity and specificity—two metrics that often trade off inversely. These observations further validate the limitations of AUROC as a sole evaluation metric, highlighting its tendency to be overly optimistic or misleading in highly imbalanced settings. While AUROC emphasizes ranking separability, it does not directly reflect clinical utility, whereas metrics like sensitivity and PPV better capture a model’s practical impact on early CA detection.

D. Feature Importance Analysis

We use permutation importance method [37] to calculate the feature importance scores for our proposed perturbed copy of the data where this feature’s values have been randomly shuffled across rows. We set number of different

permutation shuffles as 5, and the confidence level as 0.95. Top 15 important features with $p_value \leq 0.05$ are presented in Fig. 3. Our analysis reveals that key clinical indicators, such as capillary refill, total bilirubin level, and hematocrit, are among the most important predictors for pediatric cardiac arrest. Notably, factors related to hemodynamic stability and oxygenation/ventilation—including CO2 level on arterial blood gas, and FIO2,—also rank highly, emphasizing their critical role in patient monitoring. Furthermore, the inclusion of demographic factors such as sex and race highlights the multifactorial nature of cardiac arrest risk in the pediatric population. Overall, this feature importance analysis not only identifies clinical risk factors but also uncovers novel predictors that may enhance early risk detection and guide future targeted interventions.

V. CONCLUSION

Electronic health records contain a wealth of patient information that can be leveraged to study risk factors for the early detection of pediatric cardiac arrest. In this paper, we introduce PEDCA-FT, a novel multimodal fused transformer that effectively handle the heterogeneous multi-resolution EHR data. Extensive experiments on a curated pediatric cohort demonstrate the effectiveness of PEDCA-FT, indicating its potential translational impact in clinical settings. In the future, we plan to (1) extend our methodology to more diverse datasets and incorporate other modalities (*e.g.*, clinical notes, waveforms) to further enhance predictive accuracy; (2) Explore continuous risk monitoring scenarios

that enable real-time prediction updates at fixed time intervals or when new risk factor data becomes available.

ACKNOWLEDGMENT

This work was supported in part by the Nell Hodgson Woodruff School of Nursing (NHWSN) Center for Data Science of Emory University, the NHWSN High Performance Computing cluster and the NHWSN IT Department.

REFERENCES

- [1] M. E. Frazier, S. R. Brown, A. O'Halloran, T. Raymond, R. Hanna, D. E. Niles, M. Kleinman, R. M. Sutton, J. Roberts, K. Tegtmeyer, et al., "Risk factors and outcomes for recurrent paediatric in-hospital cardiac arrest: Retrospective multicenter cohort study," *Resuscitation*, vol. 169, pp. 60–66, 2021.
- [2] X. Zeng, G. Yu, Y. Lu, L. Tan, X. Wu, S. Shi, H. Duan, Q. Shu, and H. Li, "Pic, a paediatric-specific intensive care database," *Scientific data*, vol. 7, no. 1, p. 14, 2020.
- [3] R. W. Morgan, M. P. Kirschen, T. J. Kilbaugh, R. M. Sutton, and A. A. Topjian, "Pediatric in-hospital cardiac arrest and cardiopulmonary resuscitation in the united states: a review," *JAMA pediatrics*, vol. 175, no. 3, pp. 293–302, 2021.
- [4] B. D. Winters, M. M. Cvach, C. P. Bonafide, X. Hu, A. Konkani, M. F. O'Connor, J. M. Rothschild, N. M. Selby, M. M. Pelter, B. McLean, et al., "Society for critical care medicine alarm and alert fatigue task force. technological distractions (part 2): a summary of approaches to manage clinical alarms with intent to reduce alarm fatigue," *Crit Care Med*, vol. 46, no. 1, pp. 130–137, 2018.
- [5] S. Brown, J. Grunwell, Y. Wu, K. Dong, D. Bold, D. Liu, M. Fundora, X. Hu, and J. Lu, "Using machine learning to predict cardiac arrest in the pediatric cardiac intensive care unit," *Critical Care Medicine*, vol. 53, no. 1, 2025.
- [6] M. Wornow, R. Thapa, E. Steinberg, J. Fries, and N. Shah, "Ehrshot: An ehr benchmark for few-shot evaluation of foundation models," *Advances in Neural Information Processing Systems*, vol. 36, pp. 67 125–67 137, 2023.
- [7] A. Monaghan, "Detecting and managing deterioration in children," *Paediatric nursing*, vol. 17, no. 1, p. 32, 2005.
- [8] R. S. Loomba, E. G. Villarreal, S. Flores, J. S. Farias, and A. Conostas, "The inadequate oxygen delivery index and its correlation with venous saturation in the pediatric cardiac intensive care unit," *Pediatric cardiology*, pp. 1–7, 2023.
- [9] T. Chen and C. Guestrin, "Xgboost: A scalable tree boosting system," in *Proceedings of the 22nd ACM SIGKDD International Conference on Knowledge Discovery and Data Mining*, 2016, pp. 785–794.
- [10] A. Rajkumar, E. Oren, K. Chen, A. M. Dai, N. Hajaj, M. Hardt, P. J. Liu, X. Liu, J. Marcus, M. Sun, et al., "Scalable and accurate deep learning with electronic health records," *NPJ digital medicine*, vol. 1, no. 1, pp. 1–10, 2018.
- [11] M. Goswami, K. Szafer, A. Choudhry, Y. Cai, S. Li, and A. Dubrawski, "Moment: A family of open time-series foundation models," 2024. [Online]. Available: <https://arxiv.org/abs/2402.03885>
- [12] K. Rasul, A. Ashok, A. R. Williams, A. Khorasani, G. Adamopoulos, R. Bhagwatkar, M. Biloš, H. Ghonia, N. Hassen, A. Schneider, et al., "Lag-llama: Towards foundation models for time series forecasting," in *RO-FoMo: Robustness of Few-shot and Zero-shot Learning in Large Foundation Models*, 2023.
- [13] V. Ekambaram, A. Jati, P. Dayama, S. Mukherjee, N. H. Nguyen, W. M. Gifford, C. Reddy, and J. Kalagnanam, "Tiny time mixers (ttms): Fast pre-trained models for enhanced zero/few-shot forecasting of multivariate time series," *CoRR*, 2024.
- [14] X. Shi, J. Mueller, N. Erickson, M. Li, and A. Smola, "Multimodal automl on structured tables with text fields," in *8th ICML Workshop on Automated Machine Learning (AutoML)*, 2021.
- [15] J. Lu, Y. Qian, S. Zhao, Y. Xi, and C. Yang, "MuG: A multimodal classification benchmark on game data with tabular, textual, and visual fields," in *Findings of the Association for Computational Linguistics: EMNLP 2023*, Dec. 2023, pp. 5332–5346.
- [16] X. Huang, A. Khetan, M. Cvitkovic, and Z. Karnin, "Tabtransformer: Tabular data modeling using contextual embeddings," *arXiv preprint arXiv:2012.06678*, 2020.
- [17] Y. Gorishniy, I. Rubachev, V. Khurlov, and A. Babenko, "Revisiting deep learning models for tabular data," *Advances in Neural Information Processing Systems*, vol. 34, pp. 18 932–18 943, 2021.
- [18] X. Yang, A. Chen, N. PourNejatian, H. C. Shin, K. E. Smith, C. Parisien, C. Compas, C. Martin, A. B. Costa, M. G. Flores, et al., "A large language model for electronic health records," *NPJ digital medicine*, vol. 5, no. 1, p. 194, 2022.
- [19] M. Contreras, S. Kapoor, J. Zhang, A. Davidson, Y. Ren, Z. Guan, T. Ozrazgat-Baslanti, S. Nerella, A. Bihorac, and P. Rashidi, "Dellirium: A large language model for delirium prediction in the icu using structured ehr," *arXiv preprint arXiv:2410.17363*, 2024.
- [20] A. Vaswani, N. Shazeer, N. Parmar, J. Uszkoreit, L. Jones, A. N. Gomez, L. u. Kaiser, and I. Polosukhin, "Attention is all you need," in *Advances in Neural Information Processing Systems*, vol. 30, 2017.
- [21] J. Lu, S. Zhao, W. Ma, H. Shao, X. Hu, Y. Xi, and C. Yang, "Uncertainty-aware pre-trained foundation models for patient risk prediction via gaussian process," in *Companion Proceedings of the ACM Web Conference 2024*, ser. WWW '24, 2024, p. 1162–1165.
- [22] Z. Chen, C. Ding, N. Modhe, J. Lu, C. Yang, and X. Hu, "Adapting a generative pretrained transformer achieves sota performance in assessing diverse physiological functions using only photoplethysmography signals: A gpt-ppg approach," in *AAAI 2024 Spring Symposium on Clinical Foundation Models*, 2024.
- [23] W. Shi, R. Xu, Y. Zhuang, Y. Yu, J. Zhang, H. Wu, Y. Zhu, J. Ho, C. Yang, and M. D. Wang, "Ehragent: Code empowers large language models for few-shot complex tabular reasoning on electronic health records," in *Proceedings of the 2024 Conference on Empirical Methods in Natural Language Processing*, 2024, pp. 22 315–22 339.
- [24] J. D. M.-W. C. Kenton and L. K. Toutanova, "Bert: Pre-training of deep bidirectional transformers for language understanding," in *Proceedings of naacl-HLT*, vol. 1. Minneapolis, Minnesota, 2019, p. 2.
- [25] B. Jung and K. Adeli, "Clinical laboratory reference intervals in pediatrics: the caliper initiative," *Clinical biochemistry*, vol. 42, no. 16–17, pp. 1589–1595, 2009.
- [26] T.-Y. Ross and G. Dollár, "Focal loss for dense object detection," in *proceedings of the IEEE conference on computer vision and pattern recognition*, 2017, pp. 2980–2988.
- [27] N. Tomašev, N. Harris, S. Baur, A. Mottram, X. Glorot, J. W. Rae, M. Zielinski, H. Askham, A. Saraiva, V. Magliulo, et al., "Use of deep learning to develop continuous-risk models for adverse event prediction from electronic health records," *Nature Protocols*, vol. 16, no. 6, pp. 2765–2787, 2021.
- [28] H. Sakoe and S. Chiba, "Dynamic programming algorithm optimization for spoken word recognition," *IEEE transactions on acoustics, speech, and signal processing*, vol. 26, no. 1, pp. 43–49, 1978.
- [29] M. Cuturi, "Fast global alignment kernels," in *Proceedings of the 28th international conference on machine learning*, 2011, pp. 929–936.
- [30] R. Tavenard, J. Faouzi, G. Vandewiele, F. Divo, G. Androz, C. Holtz, M. Payne, R. Yurchak, M. Rußwurm, K. Kolar, and E. Woods, "Tslearn, a machine learning toolkit for time series data," *Journal of Machine Learning Research*, vol. 21, no. 118, pp. 1–6, 2020. [Online]. Available: <http://jmlr.org/papers/v21/20-091.html>
- [31] G. Ke, Q. Meng, T. Finley, T. Wang, W. Chen, W. Ma, Q. Ye, and T.-Y. Liu, "Lightgbm: A highly efficient gradient boosting decision tree," in *Advances in Neural Information Processing Systems*, 2017, pp. 3146–3154.
- [32] G. Ke, J. Zhang, Z. Xu, J. Bian, and T.-Y. Liu, "Tabnn: A universal neural network solution for tabular data," *arXiv preprint arXiv:1810.04805*, 2018.
- [33] N. Erickson, J. Mueller, A. Shirkov, H. Zhang, P. Larroy, M. Li, and A. Smola, "Autogluon-tabular: Robust and accurate automl for structured data," *arXiv preprint arXiv:2003.06505*, 2020.
- [34] Z. Wang, W. Yan, and T. Oates, "Time series classification from scratch with deep neural networks: A strong baseline," in *2017 International joint conference on neural networks (IJCNN)*. IEEE, 2017, pp. 1578–1585.
- [35] H. Liu, Z. Dai, D. So, and Q. V. Le, "Pay attention to mlps," *Advances in neural information processing systems*, vol. 34, pp. 9204–9215, 2021.
- [36] I. Oguiza, "tsai - a state-of-the-art deep learning library for time series and sequential data," Github, 2023. [Online]. Available: <https://github.com/timeseriesAI/tsai>
- [37] A. Altmann, L. Tološi, O. Sander, and T. Lengauer, "Permutation importance: a corrected feature importance measure," *Bioinformatics*, vol. 26, no. 10, pp. 1340–1347, 2010.